INVESTIGATION ON THE EFFECT OF AEROFOIL WINGTIPS ON VORTEX AND WAKE FORMATION USING PARTICLE IMAGE VELOCIMETRY

Siddharth Santhosh[1]

[1]St John's College, Cardiff

Correspondence: siddharthsanthoshcr7@gmail.com

ABSTRACT

This study investigates the effect of different aerofoil wingtips and how they result in different vortex formations. This will be analysed using P.I.V, which is Particle Image Velocimetry. Three different designs will be used: a flat plate, a filleted tip, and an endplate. Each of these designs was tested in a wind tunnel under the same testing conditions, making it a controlled experiment. The goal of this experiment is to analyse velocity planes and vorticity maps, and to see how different wingtips reduce vortex spread. The results demonstrate that using a filleted wingtip provides the best aerodynamic outcomes in a straight line, as it enables the reduction of vortex strength, provides more area for the pressure, and does not roll up into a low-velocity concentrated vortex, but has a clockwise vortex with a vorticity of -16.6(1/s). This enables a reduction in induced and pressure drag, as it reduces the pressure difference between the front and rear of the wingtip. This is because having a higher peak vorticity value represents a smaller, tighter vortex affecting a smaller volume of the surrounding environment.

INTRODUCTION

On wingtips, vortices are often formed. This is formed due to high-pressure air mixing with low-pressure air (1), as shown in the diagram below:

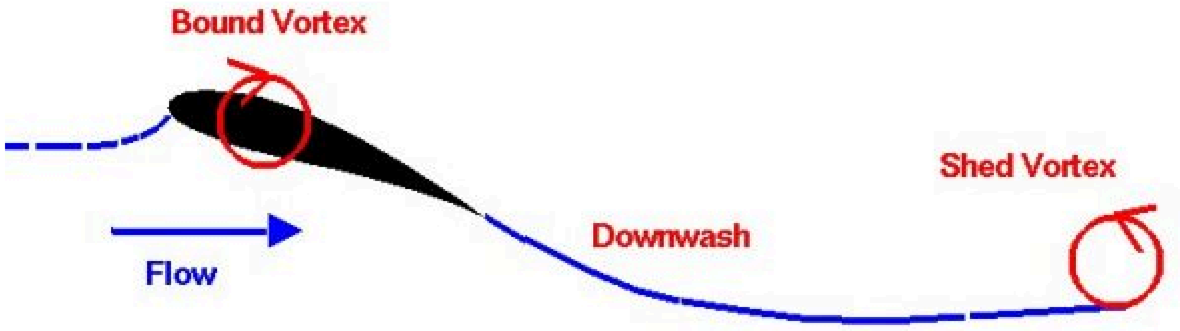

Credit: NASA Glenn Research Centre (1)

The extreme pressure differences between the lower and upper surfaces of the aerofoil drive spanwise and flow around the wingtip, resulting in a trailing vortex formation. This causes induced drag. Therefore, these wingtips are vital because they reduce induced drag.

This is a phenomenon that is directly relevant to the aerodynamic design of the wing. This is to control vortex formation for maintaining attached flow and minimizing drag.

Therefore, an important part of the aerodynamics in the wings is vortex generation to ensure that the flow attaches. Wingtips are a key influencing factor of these vortices, making them important to study using Particle Image Velocimetry (3)

Recent work has shown that passive tip geometry can drastically change the vortex velocity magnitude through decreased suction within the vortex core (9). Furthermore, wingtip geometry has been a primary source of lift-induced drag reduction in optimisations studies of fixed-wing UAVs (10).

The study aims to compare the effect of three different wingtip models on vortices, wake, and their relative strength.

METHODOLOGY

This experiment will be conducted in a wind tunnel with a PIV system, as well as various test models

Wind Tunnel Specifications:

- Testing area volume/area: $10240cm^3/320cm^2$
- Volumetric Flow Rate: $0.48m^3/s$
- Maximum Testing speed: 15 m/s
- Flow straightening method: Honeycomb Mesh
- Flow visualisation seeding: Incense smoke
- Dimensions: 16 * 21 * 21 cm.

These will be kept the same throughout each experiment, with every variable the same. This will be validated by using an anemometer to measure wind speed.

PIV system:

A laser sheet is formed using an initial laser beam, which is refracted through a cylindrical lens that forms a sheet of laser light. This allows for seeding particles to be visible using a camera (4)

The camera that will be used is an iPhone 14, which has these specifications:

- Pixels: 2532 x 1170
- Resolution: 4K
- Frames per second: 60

This is mounted approximately 10 cm away from the model, allowing for vortex formations from the wingtips of the chosen geometries.

Test Models Specifications:

- Wingspan (mm): 50
- Chord Length (mm): 50 • Wing Thickness (mm): 5.5 3D Printing Settings:

- Printer: Flashforge AD5X
- Nozzle (mm): 0.25
- Layer type/size: 0.14mm Standard @FF AD5X 0.25 Nozzle.
- Wall printing order: Outer/Inner
- Printer Speeds (mm/s): 60/150
- Infill: 15%

Experiment Specifications:

- Testing speed: 2 m/s – Ensures acceptable particle displacement between consecutive frames whilst remaining below the threshold at which mechanical vibration from the fan affects results.
- • Angle of attack – 8˚

  This was conducted at a low Reynolds number of 6768 with consistent testing parameters for low speeds (5, 11)

  $$Re = (\rho \cdot U \cdot L)/\mu = (1.225 \times 2 \times 0.05) / 1.81\times10^{-5} \approx 6,768$$

- Constant Variables:
  - Testing Airflow Speed
  - Angle of Attack
  - Frontal Surface Area
  - Wingspan
  - Chord Length
  - Geometry

While in some cases using a scientific-grade CCD camera is acceptable in PIV experiments, previous work has shown that using smartphone cameras at 60fps and 4K resolution is also acceptable (8). However, lens distortion was not applied in the study – this is a limitation.

Data Processing will be conducted using an Anaconda-Navigator environment, which encompasses OpenPIV (6). OpenPIV is an open-source particle image velocimetry toolkit implemented in Python. Recorded video frames from the iPhone 14 are converted into individual image frames and cropped to isolate the region of analysis in the laser sheet.

Velocity maps are generated by analysing the displacement of the seeded particles between the consecutive video-image frames. Where OpenPIV comes in is applying a cross-correlation algorithm, where each image is divided into interrogation windows. The displacement of the seeded particle patterns within these windows is calculated, and the velocity vectors are calculated using:

$$v = \Delta x / \Delta t$$

Where Δx represents particle displacement, and Δt represents the time difference between frames. From computed velocity maps, vorticity can be derived to quantify rotational flows. In 2-D, vorticity is seen as a spatial curl in the velocity plane, allowing us to measure the local rotation within the fluid. This means that high vorticity correlates directly with a strong vortex formation, allowing us to compare vortex strength and wingtip geometries.

The variable we will be measuring is wake and vortex formation by using the frame difference and calculating speed and different areas of the wake.

RESULTS

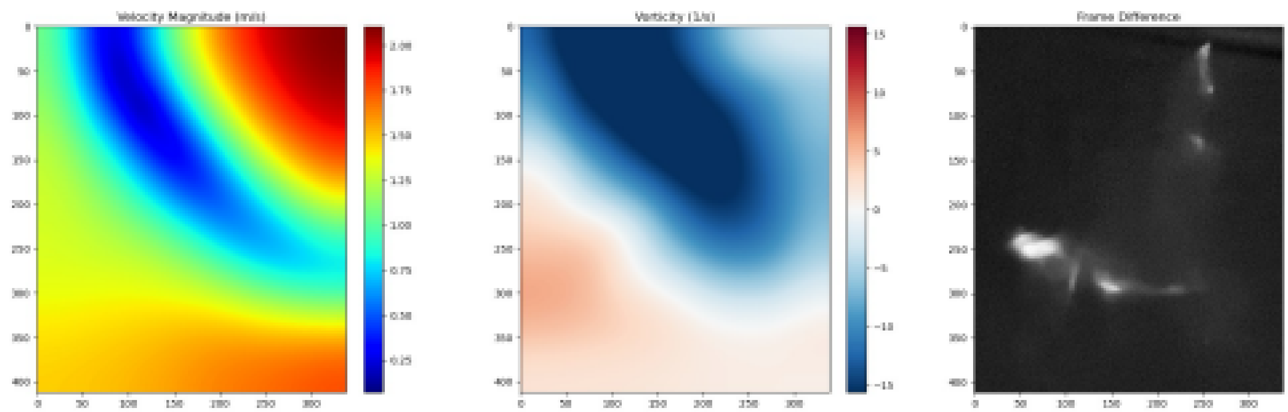

Figure 1 shows velocity magnitude, vorticity, and frame difference between frame_001.tif and frame_002.tif for the model of a flat wingtip.

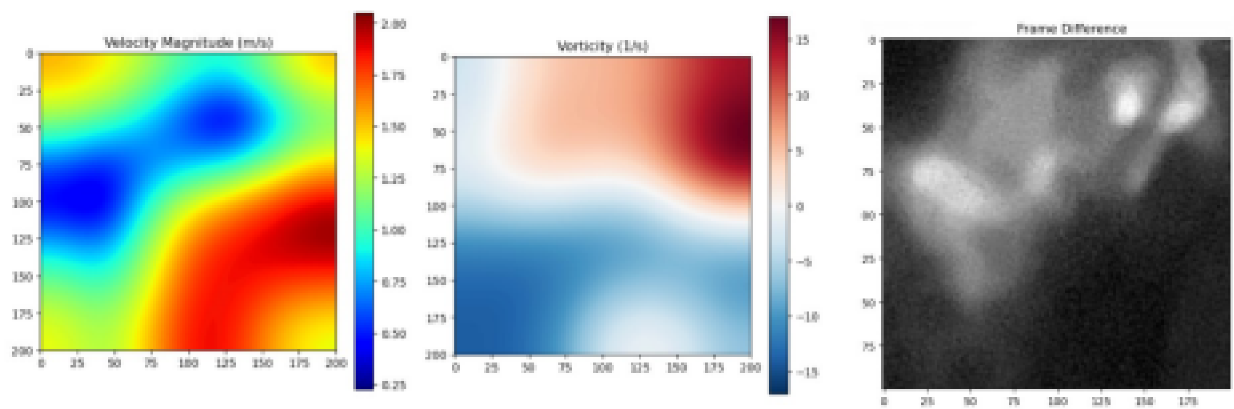

Figure 2 shows velocity magnitude, vorticity, and frame difference between frame_019.tif and frame_020.tif for the model of a filleted wingtip.

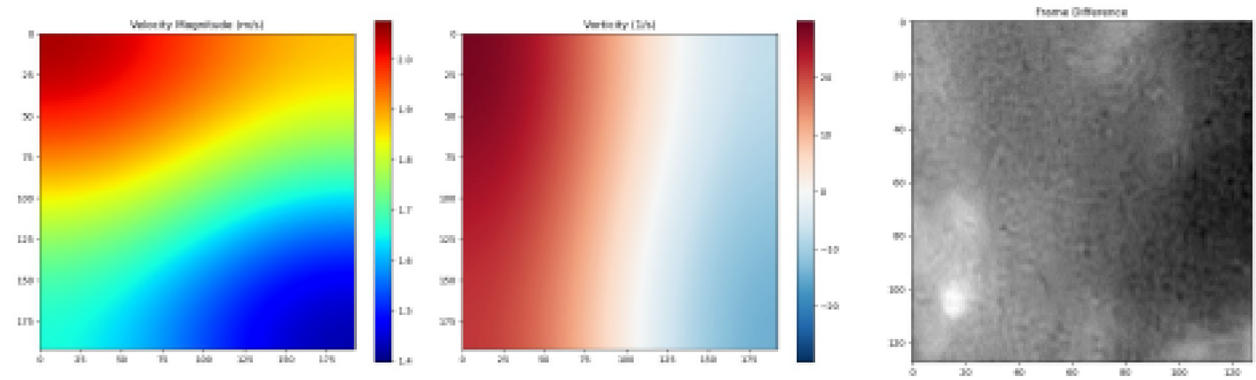

Figure 3 shows velocity magnitude, vorticity, and frame difference between frame_001.tif and frame_002.tif for the model of an endplate wingtip.

DISCUSSION

From Figure 1, we can see the correlation between the frame difference and velocity magnitude. There is also a distinct dark blue diagonal “trough” which represents low velocity. This aligns with the curved path of white streaks from the frame.

From the vorticity, we have seen a patch of dark blue representing a region of intense rotational strength. By comparing with the scale, we can see that it has a strong clockwise rotation due to it having a vorticity of -15 (1/s). This can be identified as a vortex core. The significant negative vorticity peak indicates energy dissipation associated with lift-induced drag. This means due to its strength, there is a high amount of energy loss and high drag. Therefore, we can measure the effectiveness of each design by mitigating the vortex roll-up.

From Figure 2, we can see that the correlation between the Frame Difference and Velocity Magnitude reveals a more defined flow structure. The highest regions reach approximately 2.2 m/s, matching the wind tunnel’s free stream velocity of 2.3 m/s. A visible “velocity trough” of 0.45m/s correlates with the region of wake trailing from the wing tip.

From the vorticity, we have seen that a region of negative vorticity peaking at -16.6 (1/s) indicates a clockwise vortex core. Additionally, directly above is a secondary region of positive vorticity peaking at 17 (1/s). This shows a strong vortex in an anticlockwise motion. However, since there are two streams of fluid that have moved in opposite directions relative to each other, it creates a zone of intense friction and vortex between them (7). This is known as a counter-rotating shear layer (2). You can see this visibly by the white line separating the two.

This behaviour is due to the filleted geometry acting as a transitional buffer for the high-pressure air interacting with the lower-pressure air. This allows for a longer, smoother path to travel over, thus spreading the pressure equalization over a larger surface. This
helps prevent it from rapidly rolling up into a concentrated, high-velocity spiral, such as the unfilleted wingtip.

Furthermore, having a filleted wingtip pivots the origin for the vortex. This is seen in the PIV results, where we can see a velocity deficit that is narrower and shallower compared to the control wingtip. This shows that it adheres more to the geometry, rather than accumulating into a broad, low-momentum wake region. This can be proven by the Coanda Effect (12), as a fluid (air in this case) adheres better to a curved surface than to an uncurved one. The latter is the one modelled as the control, resulting in that premature wake formation.

Although there is a higher peak, the flow is more “defined”, adhering to the geometry of the wing via the Coanda Effect: due to the curvature, the attached flow keeps momentum closer to the wing’s surface, allowing the surrounding air with high velocity to re-energise the air more rapidly. This also minimises pressure drag, as there is no significant pressure difference between the front of the wing and the rear.

Additionally, having a higher peak velocity is better because the total circulation is lower. This is because total circulation (γ)

$$\gamma = \iint \omega \, dA$$

Therefore, the higher peak vorticity has a smaller area compared to the data, and thus the total circulation is lower. This results in lower induced drag.

From Figure 3, we can see a strong diagonal gradient, which shows a velocity deficit. As the 2 m/s freestream hits the wing and the flat face of the endplate, the fluid loses its kinetic energy due to viscous friction and pressure drag. We can also see two vortex-like structures in the top left and bottom right. This shows a distinct amount of energy loss.

From the vorticity, we can see a distinct vertical split. This can be seen as a shear layer, as the high-velocity air mixes with the low-velocity air.

We do not see a single massive vortex core because, as the conflicting pressure air tries to escape, it must spill over the edges of the endplate instead. This results in two smaller, counter-rotating vortices – seen in Fig. 3 Vorticity.

CONCLUSION

In conclusion, we can see the fileted wingtip proved to be the best design in terms of aerodynamics, allowing for high-pressure air from the lower surface to transition to the upper surface over a broader area – wingtip. This provides low-pressure drag, as the low velocity wake reenergises quickly, minimising the pressure difference in the front of the wing and the rear.

However, for the endplate model, it prevented the fluid from snapping into a high intensity vortex but resulted in a large velocity deficit.

Lastly, for the control, with no additional wingtip geometries, it produced the highest level of energy dissipation and induced drag.

Therefore, for the highest efficiency, the filleted wingtip supersedes the rest. For wake management, endplates are the best as they can easily manipulate the fluid from perpendicular geometries.

Funding: This research has no external funding from other institutions and/or organisations.

Conflicts of Interest: The author(s) declare no conflicts of interests.

Data Availability Statement: "The raw PIV imagery and processed data supporting the findings of this study are available from the corresponding author upon reasonable request."

AI Usage: No AI tools were used in the conduction of this

manuscript. **REFERENCES**

1. **National Aeronautics and Space Administration (NASA)** (n.d.). *Shed vorticity*. Available at: https://www1.grc.nasa.gov/beginners-guide-to-aeronautics/shed-vorticity/ (Accessed: 25 April 2026).
2. **Moïdy, F., Pasutto, T., Daube, O., & Rossi, M.** (2004). Experimental and numerical study of the shear layer instability between two counter-rotating disks. *Journal of Fluid Mechanics*. Available at: https://www.researchgate.net/publication/231901106 (Accessed: 25 April 2026).

3. **Whitcomb, R.T.** (1976). *A design approach and selected wind-tunnel results at high subsonic speeds for wing-tip mounted winglets*. NASA Technical Note D-8260. Available at: https://ntrs.nasa.gov/citations/19760014431 (Accessed: 25 April 2026).
4. **Prasad, A.K.** (2000). Particle image velocimetry. *Current Science*, 79(1), 51-60. (Accessed: 25 April 2026).
5. **Bardera, R., Barroso, E., & Matías, J.C.** (2022). Wingtip Vortices of a Biomimetic Micro Air Vehicle. *IntechOpen*. DOI: 10.5772/intechopen.102748. Available at: https://www.intechopen.com/chapters/80381 (Accessed: 25 April 2026).
6. **Liberzon, A., et al.** (2024). *OpenPIV: A Python package for Particle Image Velocimetry*. Available at: https://github.com/OpenPIV/openpiv python (Accessed: 25 April 2026).
7. **Anderson, E.A., & Wright, C.T.** (2000). *Experimental Study of the Structure of a Wingtip Vortex*. NASA Technical Reports Server. Available at: https://ntrs.nasa.gov/citations/20000025188 (Accessed: 25 April 2026).
8. **Käufer, T., König, J., & Cierpka, C.** (2021). Stereoscopic PIV measurements using low-cost action cameras. *Experiments in Fluids*, 62, 57. DOI: 10.1007/s00348-020-03110-6. Available at: https://link.springer.com/article/10.1007/s00348-020-03110-6 (Accessed: 3 May 2026).
9. **Liu, Y., et al. (**2025). Passive control of wing-tip vortices through a grooved-tip design. *Experiments in Fluids*, 66(11), 202. DOI: 10.1007/s00348-025-04128-4. Available at: https://link.springer.com/article/10.1007/s00348-025-04128- 4 (Accessed: 9 May 2026).
10. **Almutairi, M.A., Dunning, P.D., & Maheri, A.** (2025). Winglet design for aerodynamic and performance optimization of UAVs via surrogate modelling. *Aerospace*, 12(1), 36. DOI: 10.3390/aerospace12010036. Available at: https://www.mdpi.com/2226-4310/12/1/36 (Accessed: 9 May 2026).
11. **Saravanan, P., et al.** (2025). Numerical analysis of aerodynamics performance of wingtip modifications on low Reynolds number flight. In: *Innovations in Electronic Materials*. Springer. DOI: 10.1007/978-3-031-73816-6_57. Available at: https://link.springer.com/chapter/10.1007/978-3-031-73816- 6_57 (Accessed: 9 May 2026).
12. **Nausin, M., et al.** (2023). Influence of surface curvature on the Coanda effect. *Journal of Applied Fluid Mechanics*, 16(4), 717–723. DOI: 10.47176/jafm.16.04.1583. Available at:

https://www.jafmonline.net/article_2175_77325f57a6ef1d16d1a66e5a69fcaa7f.pdf (Accessed: 9 May 2026).